J Mol Model (2015) 21: 13
DOI 10.1007/s00894-014-2568-y

ORIGINAL PAPER

Theoretical study of the reaction mechanism of CH_3NO_2 with NO_2, NO and CO: the bimolecular reactions that cannot be ignored

Ji-Dong Zhang · Li-Hua Kang · Xin-Lu Cheng

Received: 12 September 2014 / Accepted: 14 December 2014 / Published online: 24 January 2015

Abstract The intriguing decompositions of nitro-containing explosives have been attracting interest. While theoretical investigations have long been concentrated mainly on unimolecular decompositions, bimolecular reactions have received little theoretical attention. In this paper, we investigate theoretically the bimolecular reactions between nitromethane (CH_3NO_2)—the simplest nitro-containing explosive—and its decomposition products, such as NO_2, NO and CO, that are abundant during the decomposition process of CH_3NO_2. The structures and potential energy surface (PES) were explored at B3LYP/6-31G(d), B3P86/6-31G(d) and MP2/6-311+G(d,p) levels, and energies were refined using CCSD(T)/cc-pVTZ methods. Quantum chemistry calculations revealed that the title reactions possess small barriers that can be comparable to, or smaller than, that of the initial decomposition reactions of CH_3NO_2. Considering that their reactants are abundant in the decomposition process of CH_3NO_2, we consider bimolecular reactions also to be of great importance, and worthy of further investigation. Moreover, our calculations show that NO_2 can be oxidized by CH_3NO_2 to NO_3 radical, which confirms the conclusion reached formerly by Irikura and Johnson [(2006) J Phys Chem A 110:13974–13978] that NO_3 radical can be formed during the decomposition of nitramine explosives.

Keywords NO_3 · NO_2 · Nitromethane · Pyrolysis · Reaction

Electronic supplementary material The online version of this article (doi:10.1007/s00894-014-2568-y) contains supplementary material, which is available to authorized users.

J.-D. Zhang (✉)
Key Laboratory of Ecophysics and Department of Physics, School of Science, Shihezi University, Shihezi 832003, People's Republic of China
e-mail: lzzjd@126.com

L.-H. Kang
College of Chemistry and Chemical Engineering, Shihezi University, Shihezi 832003, People's Republic of China

X.-L. Cheng
Institute of Atomic and Molecular Physics, Sichuan University, Chengdu 610065, People's Republic of China

Introduction

Nitro-containing explosives are an important type of high-energy material, since they release a large amount of energy in bulk decomposition. The decompositions of nitro-containing explosives have long attracted great interest. Understanding such decomposition processes is essential to obtaining an improved model for combustion or detonation of these energetic materials [1]. Although much previous research has been done on this topic, to our knowledge, the detailed decomposition mechanism of these explosives is still complex and only partly known. The difficulty stems mainly from the ultrafast detonation and the large number of secondary reactions during the decomposition process. Nitromethane (CH_3NO_2 or NM)—a liquid-insensitive high explosive—is the simplest nitro-containing explosive, and is regarded as an important prototypical energetic material [2]. The study of CH_3NO_2 is of considerable help in understanding more complex explosives such as RDX and HMX [3], thus it is one of the most extensively studied energetic materials [2–6].

Quantum chemical calculation is a powerful theoretical tool with which to investigate the decomposition of energetic materials. It can provide the most accurate and detailed description of the reaction chemistry in the absence of empirical data. Some quantum chemical calculations have also been performed to investigate the decomposition mechanism of CH_3NO_2. However, to date, most quantum chemical studies are concerned mainly with the initial unimolecular

decomposition reactions, and research focusing on the bimolecular reactions in the decomposition process is scarce.

In recent years, some quantum chemical investigations have revealed the importance of bimolecular reactions in the decomposition processes of explosives. Irikura and Johnson [7] studied the NO_2+RDX reaction by quantum mechanics, finding that NO_2 may abstract an O atom from RDX to yield NO_3 radical and ONDNTA ($C_3H_6N_6O_5$). NO_3 radical is a dominant oxidant in the atmosphere at night, and plays an important role in atmospheric chemistry. More importantly, the barrier height of this reaction is absolutely lower than that of the pathway of the unimolecular decomposition of RDX [7]. Silva et al. [8] investigated the reaction of hydroxyl radical (HO*) with s-triazine (TAZ), both of which being decomposition products of RDX. This reaction may result in the formation of oxy-s-triazine (OST), which is a decomposition product of RDX that has been detected experimentally but for which there is as yet no explanation as to how it is formed [1, 8].

The decomposition of CH_3NO_2 is a complex process, involving many unimolecular and bimolecular reactions. It is obviously not enough that we investigate unimolecular reactions only. In this work, we aimed to investigate bimolecular secondary reactions between CH_3NO_2 and its decomposition products by quantum chemical calculations. We know that the occurrence of a chemical reaction depends to a large extent on the concentration of the reactants. NO_2, NO and CO are the main decomposition products of CH_3NO_2. As they are found with high abundance during the decomposition process, it is reasonable to believe that they can react with CH_3NO_2. Moreover, Rom et al. [5] recently performed reaxFF molecular dynamics simulations on the decomposition of CH_3NO_2, and found that at a temperature of 2500 K, NO_3 radical is a decomposition product of CH_3NO_2. Based on the study of Irikura and Johnson [7], we speculate that NO_3 radical may be formed by the NO_2+CH_3NO_2 reaction. Thus, the study presented in this paper may enhance our understanding of the decomposition of CH_3NO_2.

Computational methods

Density functional theory (DFT) methods were employed to study the reactions. All calculations were carried out with the Gaussian 09 program package [9]. The (U)B3LYP/6-31G(*d*), (U)B3P86/6-31G(*d*) and (U)MP2/6-311+G(*d*, *p*) methods were used to study the molecular geometries and vibrational frequencies of the reactants, products, intermediates, and transition states in these reactions. These methods have been employed intensively [10–14] to investigate various kinds of structures and reactions, and have proved to generate satisfactory results. Vibrational analysis was performed for each stationary point to verify whether the optimized structure is a real minimum or a saddle point structure on the potential energy surface (PES) and to provide zero-point energies (ZPEs) at the same level. The transition state obtained (TS) was confirmed by an intrinsic reaction coordinate (IRC) [15] calculation at the same level of theory corresponding to the reactants and products. In addition, single point energies were also determined using the (U)CCSD(T)/cc-PVTZ method based on the optimized geometries.

Results and discussion

Evaluating the computational approach

CH_3NO_2 is a well-studied system, and a number of studies have been directed toward elucidating the reaction details of its thermal decomposition. In this study, we investigated the reported initial decomposition reactions of CH_3NO_2 to evaluate the accuracy of the computational approach used in this paper. Reactions 1–4 are reported candidates for the initial decomposition reactions of CH_3NO_2 [4, 18–22].

$$CH_3NO_2 \rightarrow CH_3 + NO_2 \quad (1)$$

$$CH_3NO_2 \rightarrow CH_2NO_2 + H \quad (2)$$

$$CH_3NO_2 \rightarrow CH_2NOOH \quad (3)$$

$$CH_3NO_2 \rightarrow CH_3ONO \quad (4)$$

Reaction 1 results from C–N bond scission; reaction 2 is proton dissociation; reaction 3 is H intramolecular migration, and reaction 4 is nitro-nitrite isomerization. Of these, reaction 1 is a widely accepted initial reaction of the decomposition of the gas CH_3NO_2, because of its low barrier. The calculated bond dissociation energies and barriers of these reactions are listed in Table 1, together with the available data. It is clear that the results are in good agreement with the available data, which demonstrates the accuracy of our study.

Reactions between title molecules and CH_3NO_2

Next, we turned to investigate reactions between the title molecules and CH_3NO_2. The calculated molecular and transition structure energies with different methods are listed in Table S1 in the supplementary material. In Table 2, we list the barrier heights for all pathways (all energies include ZPE). Figure 1 illustrates the optimized

Table 1 The calculated bond dissociation energies (BDE, kcal mol^{-1}) and barrier heights (BH, kcal mol^{-1}) with zero-point energy (ZPE) corrections of some popular initial decomposition reactions of CH_3NO_2 with available data for comparison

	Reaction 1 (BDE)	Reaction 2 (BDE)	Reaction 3 (BH)	Reaction 4 (BH)
B3lyp/6-31G(d)	54.8	97.2	64.3	66.4
B3p86/6-31G(d)	58.6	99.7	57.3	68.6
MP2/6-311+G(d,P)	57.7	97.2	65	70.3
CCSD(T)/cc-pVTZ// B3lyp/6-31G(d)	56.4	98.9	62.6	67.1
CCSD(T)/cc-pVTZ// B3p86/6-31G(d)	56.4	98.9	62.6	67.1
CCSD(T)/cc-pVTZ// MP2/6-311+G(d,p)	57.4	99	62.6	67.3
Other works	61.9[a] 60.1[b] 58.5[c]	103.3[a] 91.9[d]	64[a]	59.2[e] 63.44[f]

[a] Theoretical calculation using G2MP2 method [4]

[b] Experimental result [18]

[c] Experimental result [19]

[d] Theoretical calculation using MP2 method [20]

[e] Theoretical calculation using UCCSD(T)/CBS [21]

[f] Theoretical calculation using UB3LYP/6-311+g(d,p) [22]

geometry structures for the reactant complex, transition states, and products of the reactions involved in this study, and Fig. 2 depicts the potential energy diagram. In the rest of the paper, the geometries discussed are based on (U)B3LYP/6-31G(d) method, and the energies are based on (U)CCSD(T)/cc-PVTZ//(U)B3LYP/6-31G(d). Moreover, we considered several spin state PES, and found that the NO_2+ CH_3NO_2 and NO+ CH_3NO_2 reactions occur in both the doublet and quartet reaction channels; the CO+ CH_3NO_2 reaction also occurs in both the singlet and triplet reaction channels. The theoretical results show that, because of the lower barrier height, all reactions in this paper occur favorably on the lower spin state surface. In the rest of the paper, the reactions discussed are on the lower spin state surface. For NO_2+ CH_3NO_2 and NO+ CH_3NO_2 reactions, the $<S^2>$ values are all very close to 0.75, which shows that the spin contamination of pure doublets states for fragment open-shell systems is negligible.

The NO_2+ CH_3NO_2 reaction

In the CH_3NO_2 molecule, two O atoms are identical, so are the three H atoms, thus we need only to consider one O atom and one H atom when we investigate the attack of NO_2. Based on this consideration, we advised three different pathway entrances for the reactions: (1) direct O-abstraction from CH_3NO_2 to form NO_3+CH_3NO, (2) direct H-abstraction by the O atom of NO_2 from CH_3NO_2 to form HONO+CH_2NO_2, and (3) direct H-abstraction by the N atom of NO_2 from CH_3NO_2 to form HNO_2+CH_2NO_2. Now, we introduce these three pathways in detail. Three attack ways result in three reaction pathways and form three different products. If NO_2 approaches the O atom of CH_3NO_2 with an N atom, an O-abstraction reaction from CH_3NO_2 resulting in NO_3 radical will occur. The reaction proceeds via transition state TS1A. In the TS1A structure, the breaking O–N bond is obviously elongated from 0.122 nm in CH_3NO_2 to 0.139 nm, while the length of the forming bond N–O is shortened to 0.156 nm. The

Table 2 The calculated barrier heights (including ZPE) of the reactions involved in this study

Reaction	Barrier height (kcal mol^{-1})					
	B3lyp/6-31 g(d)	B3p86/6-31 g(d)	Mp2/6-311+g(d,p)	CCSD(T)/cc-pVDZ// B3lyp/6-31 g(d)	CCSD(T)/cc-pVDZ// B3p86/6-31 g(d)	CCSD(T)/cc-pVDZ// Mp2/6-311+g(d,p)
NO_2+ $CH_3NO_2 \xrightarrow{TS1A}$ NO_3+CH_3NO	24.3	22.2	–	29.7	29.7	–
NO_2+ $CH_3NO_2 \xrightarrow{TS1B}$ HONO+CH_2NO_2	38.2	38.3	–	30.4	30.8	–
NO_2+ $CH_3NO_2 \xrightarrow{TS1C}$ HNO_2+CH_2NO_2	35.2	34.1	38.7	36.9	36.8	36.1
NO+ $CH_3NO_2 \xrightarrow{TS2A}$ NO_2+CH_3NO	23.6	23.0	64.5	39.1	38.8	43.1
NO+ $CH_3NO_2 \xrightarrow{TS2B}$ HON+CH_2NO_2	58.0	54.4	68.2	64.2	64.4	61.7
CO+ $CH_3NO_2 \xrightarrow{TS3A}$ NO_2+CH_3NO	41.4	38.9	44.9	47.6	47.7	49.2
CO+ $CH_3NO_2 \xrightarrow{TS3B}$ HCO+CH_2NO_2	45.2	40.8	51.9	53.3	53.5	53.3

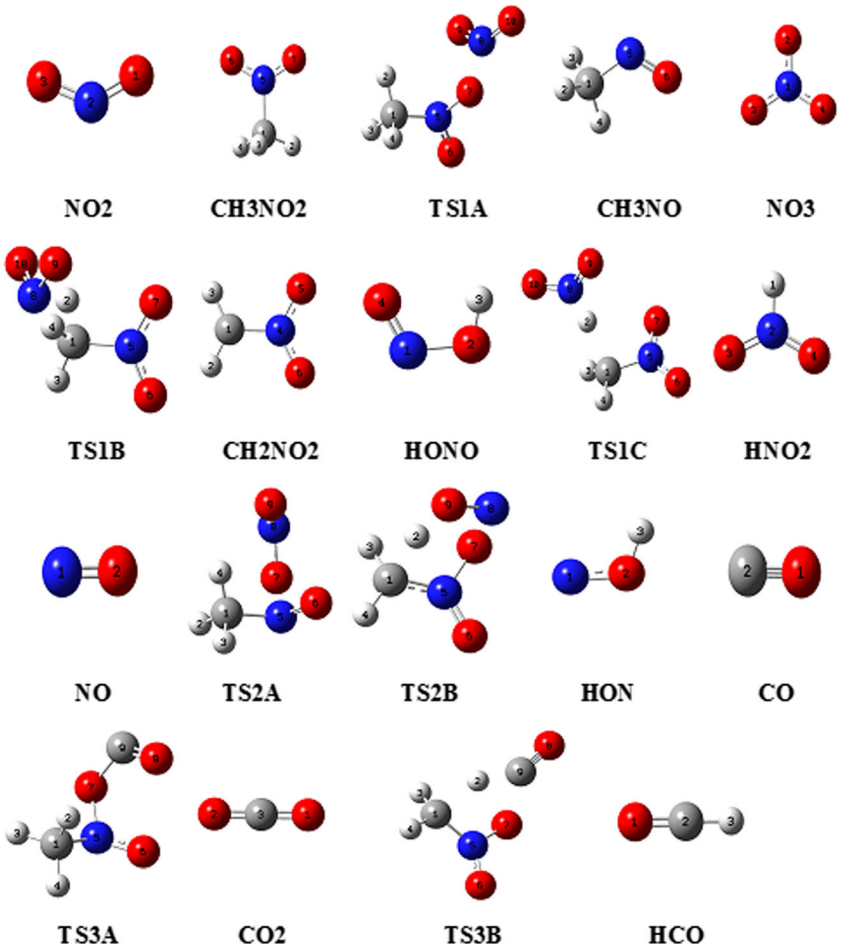

Fig. 1 B3LYP/6-31G(d) geometries of minima and transition states of the reactions involved in this study

transition state structure is characterized by an imaginary frequency 194i cm^{-1}. The products of this channel are NO_3 radical and CH_3NO. The reaction proceeds with a low barrier of 29.7 kcal mol^{-1}, and the products are 44.4 kcal mol^{-1} above the reactants, so the channel is endothermic. The thermodynamic energy requirement of the channel is smaller than that of the initial decomposition reactions of CH_3NO_2 [4, 18–22], indicating that occurrence of the channel is energetically feasible. The quantum chemistry calculations of Irikura and Johnson [7] also predicted that NO_3 radical can be formed by the reaction of NO_2+ RDX, and our calculated barrier of the channel is almost the same as reported by Irikura and Johnson (about 32.5 kcal mol^{-1}). Because the reaction is endothermic, and the reverse reaction has no barrier, it occurs more easily. This gives an explanation as to why NO_3 radical has rarely been found in former research into the decomposition of CH_3NO_2, both by experiment and theoretical calculations, with the exception of Rom's study of the decomposition of CH_3NO_2 at a high temperature of 2500 K by reaxFF molecular dynamics simulations [5]. H abstraction reactions stem from the attack of an O atom or N atom of NO_2 to an H atom of CH_3NO_2. The H atom of CH_3NO_2 can be abstracted by an O or N atom of NO_2 via transition states TS1B and TS1C respectively. In TS1B and TS1C, the forming O–H and N–H bonds are 0.122 nm and 0.112 nm, respectively. The breaking C–H bonds are elongated from 0.109 nm in CH_3NO_2 to 0.130 nm and 0.166 nm, respectively. The averaged imaginary frequency of the transition states TS1B and TS1C were calculated to be 1687i and 430i cm^{-1}. The two transition states were both verified to be the real transition state of this reaction by vibrational analysis and IRC calculations [15]. The barriers of these two H abstraction reactions were calculated to be 30.4 and 36.9 kcal mol^{-1}, lower than those reported initial decomposition reactions of CH_3NO_2 [4, 18–22]. Moreover, the products of these two reactions were less favorable in energy by 22.3 and 32 kcal mol^{-1}, respectively, than the reactants.

The above results show that H abstraction reactions are the main channel of the reaction NO_2+ CH_3NO_2. However, O abstraction has slightly higher thermodynamic energy requirements, suggesting the possibility that NO_3 might be formed during the decomposition of CH_3NO_2.

The NO+ CH_3NO_2 reaction

We found two channels for the reaction: (1) direct O-abstraction by the N atom of NO from CH_3NO_2 to form

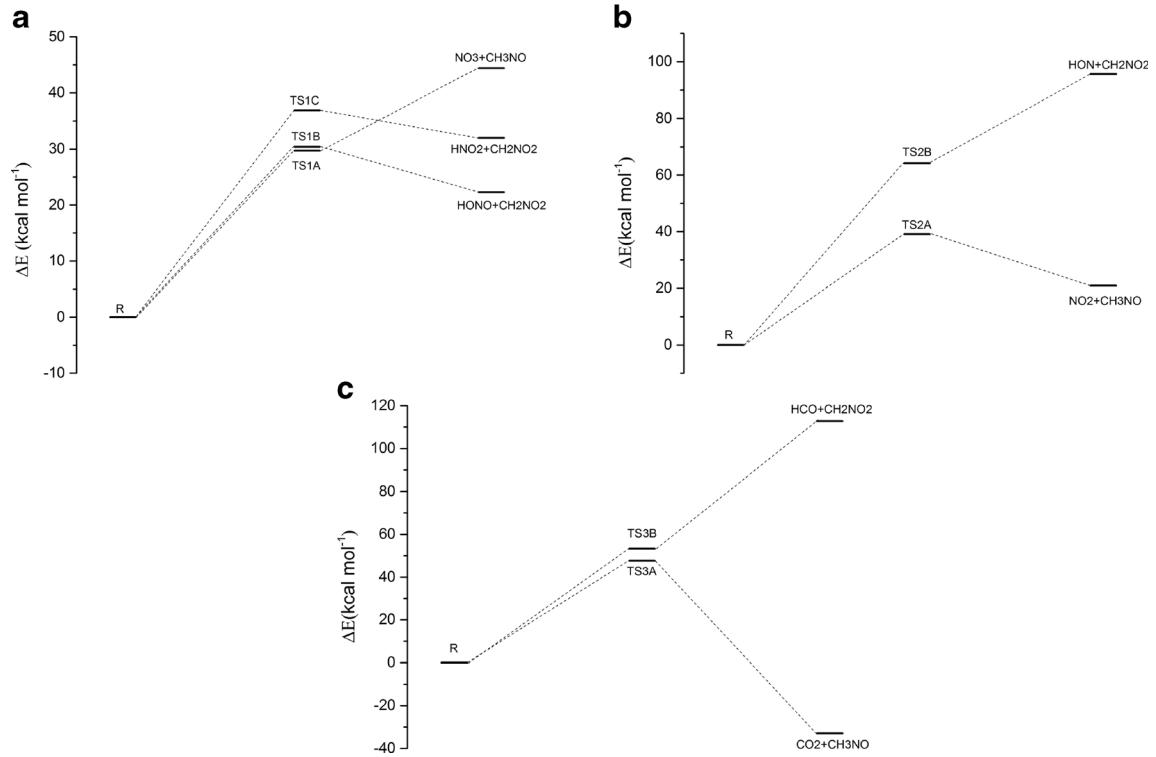

Fig. 2 Potential energy diagram for the reactions **a** $NO_2+CH_3NO_2$, **b** $NO+CH_3NO_2$ and **c** $CO+CH_3NO_2$

NO_2+CH_3NO, and (2) direct H-abstraction by the O atom of NO from CH_3NO_2 to form $HON+CH_2NO_2$. Different from NO_2, we found no H-abstraction reaction from CH_3NO_2 by the N atom of NO. The attack of the N atom in NO to an O atom of CH_3NO_2 may result in the O abstraction from CH_3NO_2. TS2A is the transition state of this process. An IRC calculation was performed to verify that the TS2A structure is the real transition state of this reaction. The results show that the starting and finishing points of the reaction correspond closely to the reactant and product in geometry and energy. TS2A is a product-like transition state with an imaginary frequency of 439i cm^{-1}. In TS2A, the O atom shifts to the N atom in NO. The forming O–N bond is 0.127 nm, and the breaking N–O bond is elongated from 0.122 nm in CH_3NO_2 to 0.197 nm. The reaction barrier for O abstraction is estimated to be 39.1 kcal mol^{-1}. The reaction will produce NO_2+CH_3NO, and the products lie 21.0 kcal mol^{-1} above the reactants in energy, suggesting that the process is slightly endothermic. Furthermore, direct attack on the H atom of CH_3NO_2 by an O atom in NO will result in an H abstraction route. The reaction proceeds via transition state TS2B with a reaction barrier of 64.2 kcal mol^{-1}. In TS2B, the H atom is transferred from C atom to O atom. The forming O–H bond is 0.109 nm, and the breaking C–H bond is elongated from 0.109 nm in CH_3NO_2 to 0.159 nm. The reaction will result in the formation of $HON+CH_2NO_2$, and the reaction is calculated to be endothermic by 95.6 kcal mol^{-1}.

Overall, the results show that the barrier of the O abstraction reaction is smaller than those for the initial decomposition reactions of CH_3NO_2 [4, 16–22], which suggests that occurrence of the secondary reaction is feasible. The H abstraction reaction seems unimportant because of its high barrier and thermodynamic energy requirements.

The CO+ CH_3NO_2 reaction

The mechanism of the $CO+CH_3NO_2$ reaction is similar to that of the $NO+CH_3NO_2$ reaction, i.e., (1) direct O-abstraction by the C atom of CO from CH_3NO_2 to form CO_2+CH_3NO, and (2) direct H-abstraction by the C atom of CO from CH_3NO_2 to form $HCO+CH_2NO_2$. The C atom of CO attacking the O atom of CH_3NO_2 may result in the O abstraction from CH_3NO_2. The reaction proceeds via transition state TS3A with an imaginary frequency of 697i cm^{-1}. In TS3A, the O atom shifts from N atom to C atom. The forming O–C bond is 0.145 nm, and the breaking N–O bond is elongated from 0.122 nm in CH_3NO_2 to 0.144 nm. The reaction barrier for O abstraction was calculated to be 47.6 kcal mol^{-1}. The products of the reaction are CO_2+CH_3NO, which are 32.9 kcal mol^{-1} below the reactants in energy. Another channel is that a C atom in CO attacks a H atom of CH_3NO_2, which will result in a H abstraction route. The reaction proceeds via transition state TS3B with a reaction barrier of 53.3 kcal mol^{-1}. In TS3B, the H atom is shifted to the C atom

in CO. The forming C–H bond is 0.133 nm, and the breaking C–H bond is elongated from 0.109 nm in CH_3NO_2 to 0.150 nm. $HCO+CH_2NO_2$ will be formed in this channel, which are higher than the reactants by 112.8 kcal mol^{-1} in energy, so it is highly endothermic.

Like the NO+ CH_3NO_2 reaction, the barrier of the O abstraction reaction is smaller than the barriers for the initial decomposition reactions of CH_3NO_2, while the H abstraction reaction has a high barrier and thermodynamic energy requirements, which means that the O abstraction reaction is the main reaction channel for the reaction of CO+ CH_3NO_2; the secondary reaction seems to be important in the decomposition reactions of CH_3NO_2.

Conclusions

Using computational chemistry methods, we studied some secondary reactions between CH_3NO_2 and its three main decomposition products NO_2, NO and CO during the decomposition process. The results show that the three molecules can react with CH_3NO_2, because the barriers of the secondary reactions are comparable to, or smaller than, the barriers of the initial decomposition reactions of CH_3NO_2. NO_2 can react with CH_3NO_2 by three channels (O abstraction, and H abstraction by N atom and O atom). The oxidation of NO_2 by CH_3NO_2 (O abstraction reaction) will produce NO_3 radical, which has rarely been found in previous research. The reactions of NO and CO with CH_3NO_2 have two channels (O abstraction, and H abstraction). O abstraction for the reactions of NO and CO with CH_3NO_2 have a significantly lower barrier than that of the initial decomposition reactions of CH_3NO_2. The results show that bimolecular reactions (secondary reactions) between CH_3NO_2 and its decomposition products are important and should not be ignored.

Acknowledgments This project was supported by the National Natural Science Foundation of China (No. 21363019).

References

1. Chakraborty D, Muller RP, Dasgupta S, Goddard WA III (2000) J Phys Chem A 104:2261–2272
2. Guo F, Cheng XL, Zhang H (2012) J Phys Chem A 116:3514–3520
3. Guo F, Cheng XL, Zhang H (2009) J Theor Comput Chem 9:315–325
4. Hu WF, He TJ, Chen DM, Liu FC (2002) J Phys Chem A 106:7294–7303
5. Rom N, Zybin SV, van Duin ACT, Goddard WA III, Zeiri Y, Katz G, Kosloff R (2011) J Phys Chem A 115:10181–10202
6. Citroni M, Datchi F, Bini R, Vaira MD, Pruzan P (2008) J Phys Chem B 112:1095–1103
7. Irikura KK, Johnson RD (2006) J Phys Chem A 110:13974–13978
8. da Silva G, Bozzelli JW, Asatryan R (2009) J Phys Chem A113: 8596–8606
9. Frisch MJ, Trucks GW, Schlegel HB, Scuseria GE, Robb MA, Cheeseman JR, Scalmani G, Barone V, Mennucci B, Petersson GA, Nakatsuji H, Caricato M, Li X, Hratchian HP, Izmaylov AF, Bloino J, Zheng G, Sonnenberg JL, Hada M, Ehara M, Toyota K, Fukuda R, Hasegawa J, Ishida M, Nakajima T, Honda Y, Kitao O, Nakai H, Vreven T, Montgomery JA Jr, Peralta JE, Ogliaro F, Bearpark M, Heyd JJ, Brothers E, Kudin KN, Staroverov VN, Kobayashi R, Normand J, Raghavachari K, Rendell A, Burant JC, Iyengar SS, Tomasi J, Cossi M, Rega N, Millam JM, Klene M, Knox JE, Cross JB, Bakken V, Adamo C, Jaramillo J, Gomperts R, Stratmann RE, Yazyev O, Austin AJ, Cammi R, Pomelli C, Ochterski JW, Martin RL, Morokuma K, Zakrzewski VG, Voth GA, Salvador P, Dannenberg JJ, Dapprich S, Daniels AD, Farkas O, Foresman JB, Ortiz JV, Cioslowski J, Fox DJ (2010) Gaussian 09, Revision B.01. Gaussian, Inc, Wallingford
10. Becke AD (1993) J Chem Phys 98:5648–5652
11. Li QS, Zhang Y, Zhang SW (2004) J Phys Chem A 108:2014–2019
12. Zhang JD, Cheng XL (2012) J Chem Phys 137:214317
13. Zhang JD, Wang HF, Xue XY, Zhang YW, Cheng XL (2012) Acta Chim Sin 70:2543–2548
14. Su XF, Cheng XL, Meng CM, Yuan XL (2009) J Hazard Mater 161: 551–558
15. Gonzalez C, Schlegel HB (1990) J Phys Chem 94:5523–5527
16. Curtiss LA, Raghavachari K, Redfern PC, Rassolov V, Pople JA (1998) J Chem Phys 109:7764–7776
17. Boboul AG, Curtiss LA, Redfern PC, Raghavachari K (1999) J Chem Phys 110:7650–7657
18. Benson SW (1976) Thermochemical Kinetics. Wiley, New York
19. Batt L, Robinson GN (1982) The chemistry of amino, nitroso, and nitro compounds and their derivatives. In: Patai S (ed) Wiley, New York
20. Mckee ML (1986) J Am Chem Soc 108:5784–5792
21. Zhu RS, Lin MC (2009) Chem Phys Lett 478:11–16
22. Homayoon Z, Bowman JM (2013) J Phys Chem A 117:11665–11672